REFERENCES

[1] D. Yavuz, "FM click shapes," *IEEE Trans. Commun. Technol.*, vol. COM-19, pp. 1271–1273, Dec. 1971.
[2] A. J. Rainal, "Theoretical duration and amplitude of an FM click," *IEEE Trans. Inform. Theory*, vol. IT-26, pp. 369–372, May 1980.
[3] S. O. Rice, "Noise in FM receivers," in *Time Series Analysis*, M. Rosenblatt, Ed. New York: Wiley, 1963.
[4] D. T. Hess, "Cycle slipping in a first-order phase-locked loop," *IEEE Trans. Commun. Technol.*, vol. COM-16, pp. 255–260, Apr. 1968.
[5] A. Glazer, "Distribution of click amplitudes," *IEEE Trans. Commun. Technol.*, vol. COM-19, pp. 539–543, Aug. 1971.
[6] H. Cramér and M. R. Leadbetter, *Stationary and Related Stochastic Processes*. New York: Wiley, 1967.
[7] G. Lindgren, "Functional limits of empirical distributions in crossing theory," *Stoch. Proc. Appl.*, vol. 5, pp. 143–149, May 1977.
[8] ——, "Model processes in nonlinear prediction with application to detection and alarm," *Ann. Prob.*, vol. 8, pp. 775–792, 1980.
[9] M. R. Leadbetter, G. Lindgren, and H. Rootzén, *Extremal Related Properties of Random Sequences and Processes*. New York: Springer-Verlag, 1983.
[10] D. Slepian, "On the zeros of Gaussian noise," in *Time Series Analysis* M. Rosenblatt, Ed. New York: Wiley, 1963.
[11] E. Bozzoni, G. Marchetti, U. Mengali, and F. Russo, "Probability density of the click duration in an ideal FM discriminator," *IEEE Trans. Aerospace Electron. Syst.*, vol. AES-6, pp. 249–252, Mar. 1970.

Nonlinear Estimation of PSK-Modulated Carrier Phase with Application to Burst Digital Transmission

ANDREW J. VITERBI, FELLOW, IEEE, AND AUDREY M. VITERBI, MEMBER, IEEE

Abstract—**Burst transmission of digital data and voice has become commonplace, particularly in satellite communication systems employing time-division multiple-access (TDMA) and packet demand-assignment multiple-access (DAMA) techniques. In TDMA systems particularly, phase estimation on each successive burst is a requirement, while bit timing and carrier frequency can be accurately tracked between bursts. A class of nonlinear estimation algorithms is described to estimate the unknown phase of a carrier which is fully modulated by *m*-ary PSK modulation. Performance of the method is determined in closed form and compared to the Cramér–Rao lower bound for the variance of the estimation error in the phase of an unmodulated carrier. Results are also obtained when the carrier frequency is imprecisely known. Finally, the effect of quantization and finite read-only-memory (ROM) implementation of the nonlinearity are determined by computer simulation.**

1. INTRODUCTION

BURST transmission of digital data and voice has become commonplace, particularly in satellite communication systems employing time-division multiple-access (TDMA) and packet demand-assignment multiple-access (DAMA) techniques. In TDMA systems particularly, phase estimation on each successive burst is a major system design issue. To assess quantitatively the magnitude of this problem, consider Fig. 1 which illustrates the baseband waveforms of a TDMA system. T is the symbol duration, T_S the slot (or burst) duration, and T_F is the frame duration, which refers to the total time allotted to transmit one slot from each active user. A single baseband waveform, as shown in Fig. 1, applies directly to binary PSK (BPSK) modulation. Two (independent) such waveforms modulating respectively the sine and cosine of the carrier frequency would generate quaternary PSK (QPSK) and, in general, l such waveforms could modulate a carrier with m-PSK modulation, where $m = 2^l$. Typically a TDMA system might support tens to hundreds of simultaneous users, with burst lengths of hundreds to tens of thousands of bits. Thus, clearly, $T \ll T_S \ll T_F$.

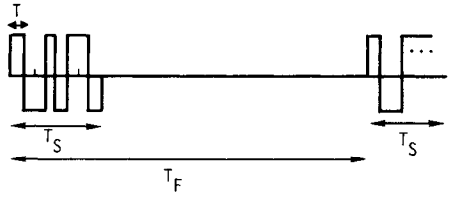

Fig. 1. Burst transmission format.

TDMA systems and networks are characterized by communication terminals which have highly accurate and controlled timing. Thus the time uncertainty Δt will be a negligibly small fraction of the symbol time T. Similarly, the carrier frequency uncertainty on any individual slot or burst Δf must be kept small compared to $1/T$ since the received energy is proportional to $[\sin(2\pi\Delta fT)/2\pi\Delta fT]^2$.

The condition $(\Delta f)T \ll 1$ can be ensured by providing reasonably stable frequency sources and by tracking

Manuscript received April 13, 1982. This work was presented at the International Symposium on Information Theory, Les Arcs, France, June 1982.

A. J. Viterbi is with M/A-COM LINKABIT, Inc., 3033 Science Park Rd., San Diego, CA 92121.

A. M. Viterbi is with the Department of Electrical Engineering and Computer Science, University of California, Berkeley, CA 94720.

0018-9448/83/0700-0543$01.00 ©1983 IEEE

frequency over several consecutive bursts. Phase accuracy, on the other hand, is almost impossible to maintain from one burst of a given user to the next. This follows from the fact that the phase difference between bursts is proportional to the frame time, i.e.,

$$(\Delta\phi)_F = 2\pi\Delta f T_F = (2\pi\Delta f T)T_F/T.$$

Even though $\Delta fT \ll 1$, the accrued phase difference between bursts may be several cycles in magnitude because $T_F/T \gg 1$. Moreover, since Δf is unknown, phase is effectively a uniform random variable at the beginning of each new burst. Note also that depending on the slot length T_S the phase variation over one slot $(\Delta\phi)_S = 2\pi\Delta f T_S$ may or may not be significant.

In any case, it is clear that if coherent communication using m-ary phase shift keying (m-PSK) is to be supported, phase must be reestimated for each successive burst (slot) of a given user. Most conventional TDMA systems provide in each slot a preamble of unmodulated carrier (or carrier modulated by a known bit pattern used also for timing update) and acquire (estimate) phase using phase-locked loop techniques. This approach is highly inefficient because the acquisition time of such loops is far in excess of the minimum required for optimal linear phase estimation.[1] This paper will show that preambles can usually be avoided and the phase can be estimated very accurately on *fully modulated m-PSK carriers* by using nonlinear estimation techniques; further, results will show that these techniques are only moderately less efficient than the optimal linear technique for estimating the phase of an unmodulated carrier.

II. Problem Framework and Comparison Standard

Fig. 2 illustrates the general structure of the phase estimator.

Let the estimation period be T_E and let it encompass N_E m-ary symbols, where $T_E = N_E T$. T_E may equal the burst (slot) length T_S or it may be less if $(\Delta\phi)_S$ is not sufficiently small. Suppose we wish to estimate the phase at the midpoint of the estimation interval and we let $N_E = 2N + 1$, where N is the number of samples before and after the sample whose phase is to be estimated. In this context and in the presence of additive white Gaussian noise (AWGN) and zero frequency uncertainty, Fig. 2 with the dotted box eliminated (so that $x_n' = x_n, y_n' = y_n$) represents the optimal (maximum likelihood) estimator for $m = 1$, $\Delta f = 0$ which corresponds to an *unmodulated* carrier.[2] The optimality of this phase estimator is well established [3]; the estimate is unbiased and the variance of the phase estimate is given by

$$\operatorname{var}(\hat{\theta}(1)) = \frac{1}{(2N+1)\gamma}\left[1 + O(2N+1)^{-1}\right], \quad (1)$$

where $\gamma = 2E_s/N_0$, E_s is the symbol energy, and N_0 is the one-sided noise spectral density. Equation (1) corresponds to the Cramér–Rao lower bound (CRB) for an efficient estimate.

Obviously, if the carrier is phase modulated to one of m discrete phases, the above linear estimator is useless since during each successive symbol the phase takes on a different value. Suppose, however, that in the dotted box we insert the two-dimensional (complex) nonlinear function

$$x_n' + iy_n' = F(\rho_n)e^{im\phi_n}, \quad (2)$$

where $\rho_n = \sqrt{x_n^2 + y_n^2}$ and $\phi_n = \tan^{-1}(y_n/x_n)$.

In words, for each symbol we perform a rectangular-to-polar transformation; multiply phase ϕ_n by m and perform an arbitrary nonlinear transformation on ρ_n; and finally perform a polar-to-rectangular transformation on the result.[3] While, we could consider a more general nonlinearity using a nonlinear function of phase as well in (2), its value and complexity does not appear to be justifiable.

Multiplying the phase by m, along with the final operation of dividing the $\tan^{-1}$ function by m, gives rise to an m-fold ambiguity in the phase estimate. A practical m-PSK modulation system adjusts for this by coding the data transitions, rather then the data itself (which is called differential encoding), and performing the inverse function of differential decoding at the receiver. This is accomplished, for example, in QPSK by having the symbol pair "00" dictate no phase change, "01" a phase shift of $\pi/2$, "11" a shift of π, and "10" a shift of $3\pi/2$, with the obvious generalization for m-PSK modulation. It does require transmission of an additional initial (unmodulated) phase symbol per burst and it results in an approximate doubling of the bit error rate, since each symbol demodulation error gives rise to two transition errors upon differential decoding. The same technique can be used even if the symbols are forward error-correction encoded and decoded (after differential encoding and before differential decoding, respectively) through use of a transparent code [4]. Alternatively, if nontransparent codes are used, decoder metrics can be used to search for the correct phase synchronization [4], [5].

We shall show in the subsequent sections that for m-PSK carriers, with appropriately chosen $F(\rho)$, this estimator performs nearly as well as the linear estimator for unmodulated carriers at high E_s/N_0, and with only moderate degradation for $E_s/N_0 > 3$ dB.

III. Major Results

For the m-PSK modulated waveform let $\hat{\theta}_n(m)$ denote the estimator for the nth symbol phase of a symmetric

[1] Departures from this approach are packet satellite modems which perform nearly optimal estimation of unknown frequency, phase, and time-of-arrival using a preamble [1], [2].

[2] Clearly in this case, division of $T_E = (2N+1)T$ into symbol intervals is artificial, and obviously

$$\sum_{n=-N}^{N} \int_{(n-1/2)T}^{(n+1/2)T} x(t)\,dt = \int_{-T_E/2}^{T_E/2} x(t)\,dt.$$

This notation is used only to establish a framework for comparison.

[3] We avoid describing the nonlinearity in this manner in Fig. 2, because in a practical implementation it becomes a read-only-memory, transforming a quantized 2-dimensional vector into another such vector (see Section V).

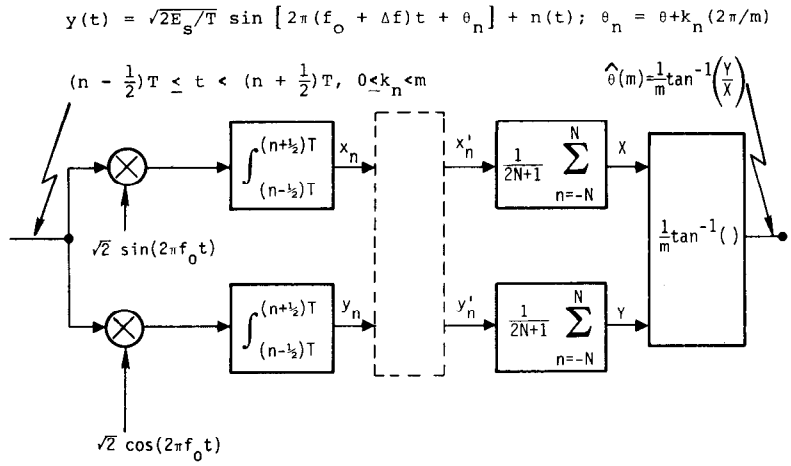

Fig. 2. Basic phase estimator for m-PSK carriers.

estimation interval ($-N \leqslant n \leqslant N$). It is easily shown that the carrier phase estimate of the middle symbol ($n = 0$), which lies in the interval $-T/2 < t < T/2$, is unbiased. For the nth symbol ($-N \leqslant n \leqslant N$) in the symmetric estimation interval of duration $T_E = (2N + 1)T$, the bias, in terms of the frequency error Δf and symbol time T, is

$$E[\hat{\theta}_n(m)] = 2\pi n(\Delta f)T, \qquad -N \leqslant n \leqslant N. \tag{3}$$

Obviously if the estimation period T_E is much less than the slot period T_s, all but the first and last N symbol estimates can be made unbiased by overlapping estimation periods, that is, by using the preceding and succeeding N symbols to estimate each symbol phase (except for the first and last N) individually. The resulting estimates are not independent, but they are unbiased. The disadvantage is that this requires approximately $(2N + 1)$ as many operations as performing a single estimate for all the $2N + 1$ symbols in the interval.

The key result is an expression for the variance of the estimator, $\text{var}[\hat{\theta}_n(m)]$, which is independent of n. We first give this for an arbitrary nonlinear function of amplitude $F(\rho)$ in terms of frequency error Δf, and then we give specific results for selected $F(\rho)$. Then, we express the result in terms of the variance for the linear case ($m = 1$) with $\Delta f = 0$ which is the Cramér–Rao lower bound (CRB).

We define, using (1) and ignoring terms of $O(2N + 1)^{-1}$,

$$\Gamma(m, \Delta f) = \frac{\text{var}[\hat{\theta}(m)|\Delta f]}{\text{var}[\hat{\theta}(1)|\Delta f = 0]} \sim \frac{\text{var}[\hat{\theta}(m)|\Delta f]}{[(2N + 1)\gamma]^{-1}}, \tag{4}$$

and we show in Appendix A that for general $F(\rho)$

$$\frac{2m^2\Gamma'(m, \Delta')}{\gamma} = \frac{\left(E(F^2(\rho)) - [E(F(\rho)\cos\epsilon')]^2\right)[1 - S_N(2\Delta')] + \left(E(F^2(\rho)) - E(F^2(\rho)\cos 2\epsilon')\right)S_N(2\Delta')}{[E(F(\rho)\cos\epsilon')]^2 S_N^2(\Delta')} \tag{5}$$

where $\Gamma'(m, \Delta') = \Gamma(m, \Delta f)$, $\Delta' = m(\Delta f)T$, $\epsilon' = m\epsilon$, and ρ and ϵ are random variables described by the joint probability density function[4]

$$p(\rho, \epsilon) = \frac{\rho}{\sigma^2} \exp - \left(\frac{\rho^2}{2\sigma^2} + \frac{\gamma}{2} - \frac{\rho\sqrt{\gamma}\cos\epsilon}{\sigma}\right) \tag{6}$$

[4]Note that σ^2 is the variance of the real and the imaginary part of each sample. Thus $\sigma^2 = (N_0/2)T$.

and where

$$S_N(\Delta') \triangleq \frac{1}{2N + 1}\left[\frac{\sin[(2N + 1)\pi\Delta']}{\sin(\pi\Delta')}\right]. \tag{7}$$

For $\Delta f = 0$, then $S_N(\Delta') = 1$ and (5) reduces, of course, to

$$\frac{2m^2\Gamma'(m, 0)}{\gamma} = \frac{E[F^2(\rho)] - E[F^2(\rho)\cos 2\epsilon']}{[E(F(\rho)\cos\epsilon')]^2}. \tag{8}$$

The needed expectations have been obtained in closed form only for the cases $F(\rho) = \rho^k$, where k and m are both even and $k \leqslant m$. (Restricting m to be even is hardly much of a limitation; we are usually interested only in m-PSK where m is a power of two.)

It is shown in Appendix B that for $F(\rho) = \rho^k$, k even,

$$E\left(\frac{\rho^{2k}}{\sigma^{2k}}\cos 2\epsilon'\right) = \gamma^k \sum_{n=0}^{m+k} n!\binom{m + k}{n}\binom{m - k + n - 1}{n}\left(\frac{-2}{\gamma}\right)^n + (-1)^{m+k+1}2^k e^{-\gamma/2}\left(\frac{2}{\gamma}\right)^{k+1} \cdot \sum_{n=0}^{m-k-1}\binom{m + k + n}{n}\frac{(m + k)!}{(m - k - n - 1)!}\left(\frac{2}{\gamma}\right)^n, \qquad k \leqslant m - 2, \tag{9a}$$

$$E\left(\frac{\rho^{2k}}{\sigma^{2k}}\right) = \sum_{n=0}^{k}\binom{k}{n}^2 \gamma^{k-n}2^n n!, \qquad k = m. \tag{9b}$$

Combining (5) and (9) for arbitrary frequency error, or (8) and (9) for zero frequency error, yields results for $F(\rho) = \rho^k$, $k \leqslant m$, and k and m both even. Note also that for $k = m$, the nonlinearity reduces to $x' + iy' = (x + iy)^m$.

These analytical results are shown graphically for QPSK ($m = 4$) in Figs. 3 and 4. The first shows, for zero frequency error, the degradation $-10\log\Gamma(4, 0)$, as a function of

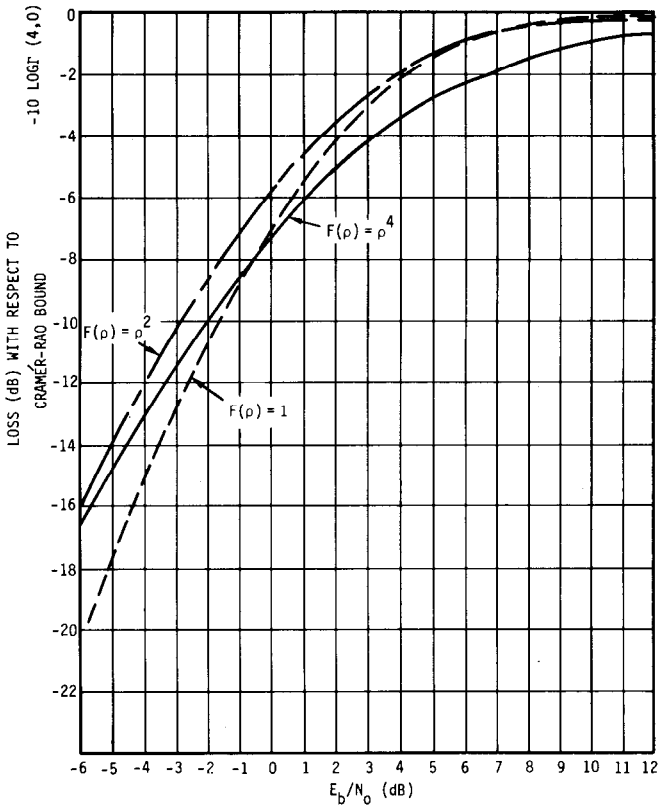

Fig. 3. Performance of QPSK phase estimator as a function of E_b/N_0.

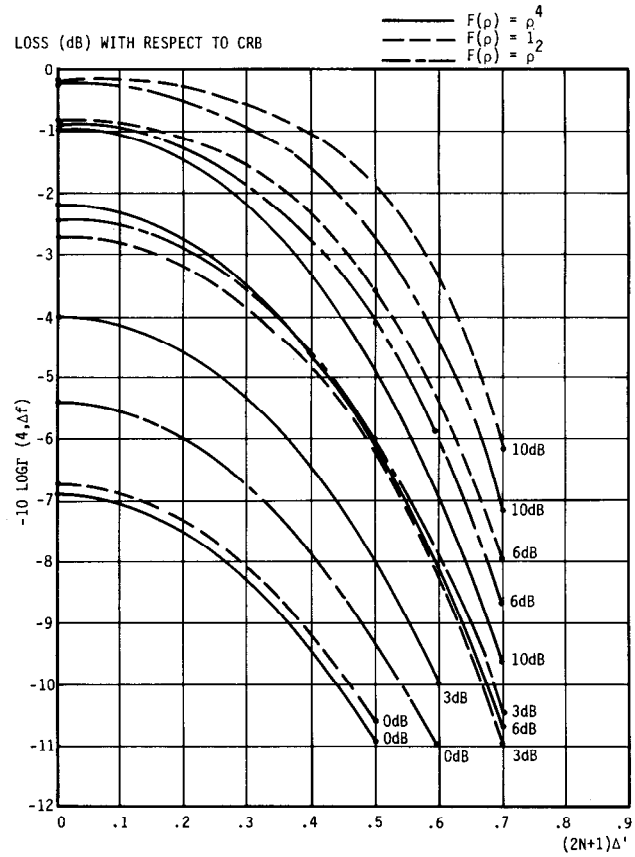

Fig. 4. Performance of QPSK phase estimator as a function of $(2N+1)\Delta'$ $(\Delta' = 4(\Delta f)T)$ $(N = 8)$.

$E_b/N_0 = \gamma/4$ for $F(\rho) = 1, \rho^2$, and ρ^4, i.e., $k = 0, 2$, and 4. The second shows $-10\log\Gamma(4, \Delta f)$ as a function of normalized frequency error $(2N+1)\Delta'$ for several values of E_b/N_0, $N = 8$, and for $F(\rho) = 1, \rho^2$, and ρ^4.

IV. Interpretation of Results and Some Limiting Cases

We note from Fig. 3 that for zero frequency uncertainty at asymptotically low E_b/N_0 the fourth power nonlinearity appears to be optimum. Such a result can be derived analytically [6]. At very high E_b/N_0, both $F(\rho) = 1$ and $F(\rho) = \rho^2$ seem to approach the same behavior. This can be verified by expanding (9a) and (9b) in a series in $1/\gamma$ and inserting these in (8). The results are

$$\Gamma(m,0) = 1 + \frac{1}{\gamma}(k-1)^2 + O\left(\frac{1}{\gamma^2}\right),$$

$$F(\rho) = \rho^k, \qquad k \leqslant m \text{ even.} \tag{10}$$

Hence

$$\Gamma(4,0) = \begin{cases} 1 + \dfrac{1}{\gamma} + O\left(\dfrac{1}{\gamma^2}\right), & F(\rho) = \rho^0 \text{ and } \rho^2; \\ 1 + \dfrac{9}{\gamma} + O\left(\dfrac{1}{\gamma^2}\right), & F(\rho) = \rho^4. \end{cases}$$

Note also that in almost the entire region of interest -6 dB $\leqslant E_b/N_0 \leqslant 6$ dB, $F(\rho) = \rho^2$ dominates for even power nonlinearities.

For nonzero frequency error, as shown by Fig. 4, the zeroth power nonlinearity is best at $E_b/N_0 \gtrsim 6$ dB, but at low $E_b/N_0 \lesssim 0$ dB, $F(\rho) = \rho^2$ is best. In all cases shown, $F(\rho) = \rho^4$ is worst, although the difference becomes much less for low E_b/N_0. The obvious advantage of using $F(\rho) = \rho^0 = 1$ is that automatic gain control (AGC) becomes unnecessary, for the nonlinearity can be implemented by a bandpass limiter.

The lack of analytical closed-form results for odd power nonlinearities, and more important, for quantized nonlinear functions (as well as the desire to validate the above results, which involved dropping higher order terms in the $\tan^{-1}$ nonlinearity) leads us to seek verification and extension of these results by simulations, as discussed in the next section.

V. Simulations and Practical Digital Implementations

For zero frequency error, Fig. 5 illustrates the result of a 10 000 independent sample simulation for $m = 4$, $N = 8$, and $\Delta f = 0$. The uppermost curve is the theoretical result for $F(\rho) = \rho^2$ taken from Fig. 3. The curves closest to this represent simulations for $F(\rho) = \rho^2$ and $F(\rho) = \rho$ performed for all even integer values of E_b/N_0 between -6 dB and $+10$ dB. The simulation results for $F(\rho) = \rho^2$ are very close (within 0.5 dB) to the analytical results at high E_b/N_0. The small degradation in the simulated results is

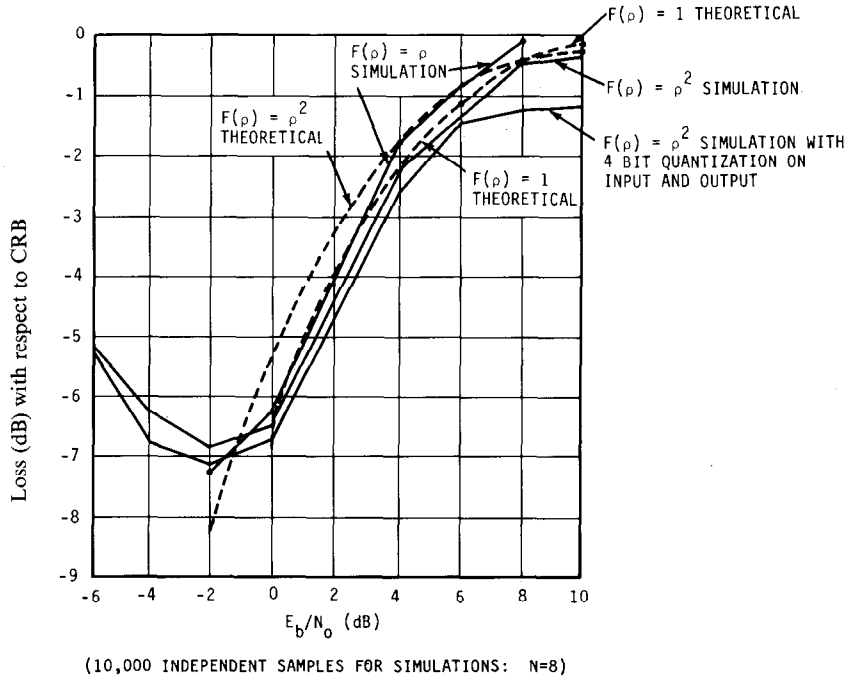

Fig. 5. Degradation of phase error for $F(\rho) = \rho^2$, ρ, and 1.

due to our optimistic dropping of $O(1/N)$ terms (and would be much smaller for $N \gg 8$). At low E_b/N_0, the turn around in the curves is due to the fact that the Cramér–Rao bound (CRB) yields $\text{var}(\hat{\theta}) \simeq 1/(2N+1)\gamma$ no matter how small γ may be, while in reality, the variance is actually bound above by that of a uniform phase distribution over the interval $-\pi/4 < \hat{\theta} < \pi/4$, which is

$$\text{var}(\hat{\theta}) \leqslant \frac{(\pi/4)^2}{3}, \tag{11}$$

so that for very small E_b/N_0, $\Gamma \to (\text{constant} \, x\gamma)$ and $-10 \log \Gamma \sim (\text{constant} \; -10 \log E_b/N_0)$, which eventually will become positive. Hence the theoretical results are meaningless for extremely low E_b/N_0. Note, however, that Γ is only the degradation factor relative to the CRB and $\text{var}(\hat{\theta})$ is a monotonically increasing function of $1/\gamma$, limited only by the uniform bound (11) as $\gamma \to 0$.

The simulation of $F(\rho) = \rho$, also shown in Fig. 5, appears to be slightly better than that of ρ^2 for high E_b/N_0 and slightly worse for $E_b/N_0 < -0.5$ dB. The high E_b/N_0 optimal behavior might be suggested by (10), even though that expression only applies for even k.

Of greater practical interest is the lowest curve of Fig. 5. This is the result of a 10 000 independent sample simulation (using the same noise samples as the previously described simulation as a control) for a nonlinearity implemented using two A/D converters for x and y and a read-only-memory (ROM) for generating x' and y', (Fig. 6.) All quantities are 4-bit quantized so that the 2-dimensional nonlinearity may be implemented, exploiting symmetry, as a $2^{2q-1} \times 2r = 128 \times 8$ ROM.

The results are impressive, showing negligible additional degradation loss at lower E_b/N_0 values and only 1 dB loss

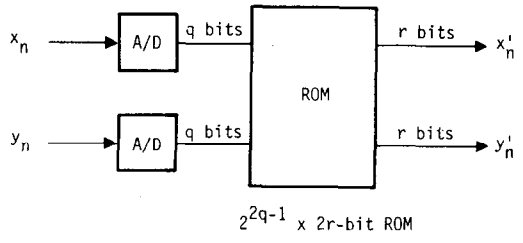

Fig. 6. Practical implementation of $x' + iy' = F(\rho)e^{im\phi}$.

even at $E_b/N_0 = 10$ dB. The additional loss is expected to be greater at higher E_b/N_0, for there the quantization error dominates other noise-related estimation errors. This quantization loss can be significantly reduced at high E_b/N_0 by increasing the quantization accuracy (q bits) at the input of the ROM (output of the A/D converter). At 10 dB the loss is less than 0.5 dB for $q = 5$ bits and unnoticeable at $q = 6$ bits. Of course, increase of q by 1-bit quadruples the size of the ROM.

Quantized performance in the presence of nonzero frequency error was also simulated for $F(\rho) = 1$, ρ, and ρ^2 with the results shown in Fig. 7. Here 50 000 samples were used, where each sample estimated is based on the eight preceding and succeeding symbols. The resulting estimates are then not independent, but at least the accuracy considerably exceeds that of 3000 independent samples.

VI. Conclusion

Using a symmetric estimation interval of N phase symbols before and N after the m-PSK modulated symbol whose (unmodulated) carrier phase is to be estimated, the estimator of Fig. 2 is unbiased and has the variance

$$\text{var}\left[\hat{\theta}(m)\right] = \frac{1}{(2N+1)\gamma}\Gamma(m, \Delta f),$$

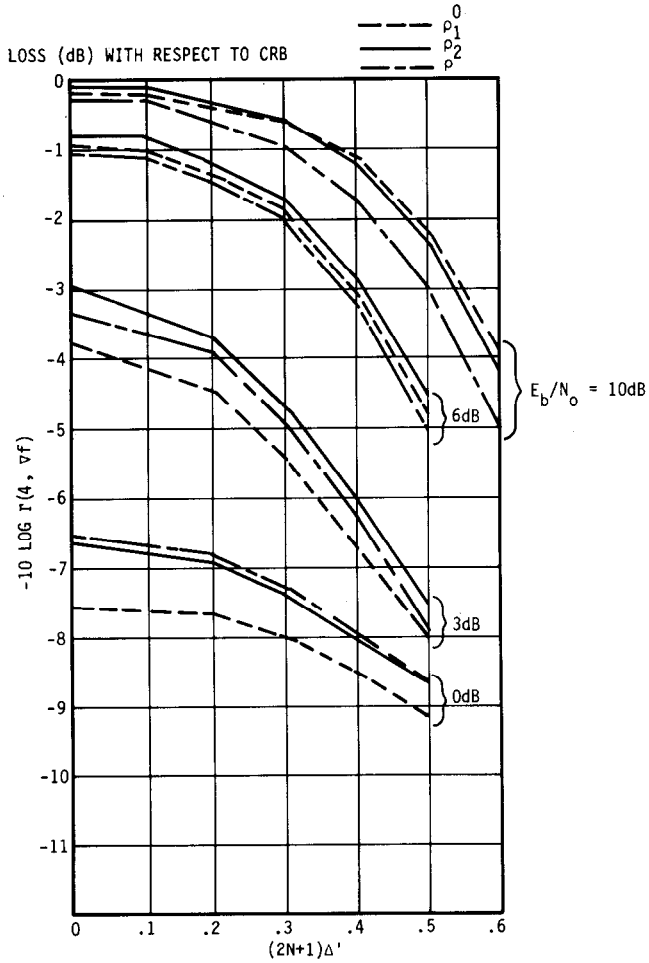

Fig. 7. Simulations with frequency error for $F(\rho) = 1, \rho, \rho^2$ $(N = 8)$.

where the degradation factor Γ is obtained analytically for even m and nonlinearities of the form

$$x' + iy' = \rho^k e^{im\phi}, \qquad k \text{ even } (k \leqslant m),$$

where ρ is the input (polar) magnitude and ϕ its phase.

In most cases, degradation is so small (a few dB) that further optimization of the estimator seems unnecessary. This is particularly true if N can be made sufficiently large to compensate for any degradation (which requires, of course, that Δf be sufficiently small such that $m(2N + 1)\Delta f$ is small compared to unity).

The present results (for zero frequency error) bear a considerable resemblance to the steady-state phase error variance of a phase locked loop with appropriate nonlinearity (i.e., a Costas-loop or some generalization thereof). In fact, for $k = m$ the variance expression (9b) is identical to that of m-ary Costas loop [6]. It should be noted, however, that in the present case no loop settling or acquisition time is required. For very small Δf, therefore, this procedure is much preferable for burst transmission, since it can obtain accurate phase estimates from virtually the first symbol of the burst. To maintain Δf small from one burst to the next, frequency tracking is required, of course, as well as stable sources at transmitter and receiver.

Appendix A

General Nonlinearity with Frequency Uncertainty

Suppose the dotted box of Fig. 2 is replaced by the nonlinearity

$$x_n' + iy_n' = F(\rho_n)e^{im\phi_n}$$

where

$$\rho_n = \sqrt{x_n^2 + y_n^2}, \quad e^{i\phi_n} = \left(\frac{x_n + iy_n}{\sqrt{x_n^2 + y_n^2}}\right); \tag{A1}$$

the phase for the nth symbol, for a frequency error Δf, is given by

$$\phi_n = \theta + 2\pi n(\Delta f)T + \epsilon_n + k_n(2\pi/m); \tag{A2}$$

ϵ_n is the noise induced phase error for the nth symbol, and the sequence is independent identically distributed.

The phase estimate obtained by the estimator of Fig. 2 for the central symbol $(n = 0)$ is easily shown to be unbiased. After accumulation over $(2N + 1)$ symbols, the phase error is

$$\epsilon = \frac{1}{m}\tan^{-1}\left[\frac{\frac{1}{2N+1}\sum_{n=-N}^{N} F(\rho_n)\sin m(\epsilon_n + 2\pi n\Delta fT)}{\frac{1}{2N+1}\sum_{n=-N}^{N} F(\rho_n)\cos m(\epsilon_n + 2\pi n\Delta fT)}\right]. \tag{A3}$$

While $E(\sin m\epsilon_n) = 0$, $E(\cos m\epsilon_n) \leqslant 1$, so that the mean of the denominator is a function of the noise statistics.

If we define

$$\epsilon_n' = m\epsilon_n$$
$$\Delta' = m(\Delta f)T \tag{A4}$$

and

$$\eta = \frac{1}{2N+1}\sum_{n=-N}^{N} E[F(\rho_n)\cos(\epsilon_n' + 2\pi n\Delta')]$$
$$\xi_n = F(\rho_n)\sin(\epsilon_n' + 2\pi n\Delta')$$
$$\zeta_n = F(\rho_n)\cos(\epsilon_n' + 2\pi n\Delta') - \eta;$$

it follows that

$$\epsilon = \frac{1}{m}\tan^{-1}\left[\frac{\frac{1}{2N+1}\sum_{n=-N}^{N}\xi_n}{\eta + \frac{1}{2N+1}\sum_{n=-N}^{N}\zeta_n}\right]. \tag{A5}$$

It follows by definition of η that

$$E\left(\sum_{n=-N}^{N}\zeta_n\right) = 0.$$

while using (6),

$$E\left(\sum_{n=-N}^{N}\xi_n\right)=E\left[\sum_{n=-N}^{N}F(\rho_n)\sin(\epsilon'_n+2\pi n\Delta')\right]$$
$$=\sum_{n=-N}^{N}\int_0^\infty F(\rho_n)\frac{\rho_n}{\sigma_n}\exp\left\{-\left(\frac{\rho_n^2}{2\sigma^2}+\frac{\gamma}{2}\right)\right\}$$
$$\cdot\int_{-\pi}^{\pi}\sin(\epsilon'_n+2\pi n\Delta')\exp\left(\frac{\rho\sqrt{\gamma}}{\sigma}\cos\epsilon'_n\right)d\epsilon'_n\,d\rho_n$$
$$=\sum_{n=-N}^{N}\int_0^\infty F(\rho_n)\cos\epsilon'_n\frac{\rho_n}{\sigma^2}$$
$$\cdot\exp-\left(\frac{\rho_n^2}{2\sigma^2}+\frac{\gamma}{2}-\frac{\rho_n\sqrt{\gamma}}{\sigma}\cos\epsilon'_n\right)d\epsilon'_n\,d\rho_n\sin 2\pi n\Delta'=0.$$

Proceeding similarly,

$$\operatorname{cov}\left(\sum\xi_n,\sum\zeta_k\right)=E\left[\frac{1}{2}\sum_{n=-N}^{N}F^2(\rho_n)\sin(2\epsilon'_n+4\pi n\Delta')\right]=0.$$

Thus

$$\epsilon\approx\frac{1}{m\eta}\left[\frac{1}{2N+1}\sum_{n=-N}^{N}\xi_n\left(1-\frac{1}{(2N+1)\eta}\sum_{n=-N}^{N}\zeta_n+\cdots\right)\right]. \tag{A6}$$

Since all variables are uncorrelated and the estimate $\hat{\theta}$ is unbiased,

$$\operatorname{var}(\hat{\theta})=\operatorname{var}(\epsilon)=\frac{E\left(\sum\xi_n^2\right)}{(2N+1)^2m^2\eta^2}\left[1+O(2N+1)^{-1}\right], \tag{A7}$$

then

$$\eta=\frac{1}{2N+1}E\sum_{n=-N}^{N}F(\rho_n)\cos(\epsilon'_n+2\pi n\Delta')$$
$$=\frac{1}{2N+1}\sum_{n=-N}^{N}E\left[F(\rho_n)\cos\epsilon'_n\right]\cos(2\pi n\Delta')$$
$$=E\left[F(\rho)\cos\epsilon'\right]S_N(\Delta'), \tag{A8}$$

where

$$S_N(\Delta)=\frac{1}{2N+1}\sum_{n=-N}^{N}\cos(2\pi n\Delta')=\frac{\sin\left[(2N+1)\pi\Delta'\right]}{(2N+1)\sin(\pi\Delta')}. \tag{A9}$$

Since for different symbols ρ_n and ϵ_n are independent of ρ_j and ϵ_j,

$$\frac{1}{2N+1}E\left(\sum\xi_n\right)^2$$
$$=\frac{1}{2N+1}E\left[\sum_{n=-N}^{N}F(\rho_n)\sin(\epsilon'_n+2\pi n\Delta')\right]^2$$
$$=\frac{1}{2N+1}E\left[\sum_{n=-N}^{N}F(\rho_n)\sin(\epsilon'_n+2\pi n\Delta')\right]$$
$$\cdot E\left[\sum_{j=-N}^{N}F(\rho_j)\sin(\epsilon'_j+2\pi j\Delta')\right]$$
$$+\frac{1}{2N+1}\left[\sum_{n=-N}^{N}E\left[F^2(\rho_n)\sin^2(\epsilon'_n+2\pi n\Delta')\right]\right.$$
$$\left.-\left\{E\left[F(\rho_n)\sin(\epsilon'_n+2\pi n\Delta')\right]\right\}^2\right]. \tag{A10}$$

The first term equals zero, while

$$\frac{1}{2N+1}\sum_{n=-N}^{N}E\left[F^2(\rho_n)\sin^2(\epsilon'_n+2\pi n\Delta')\right]$$
$$=\frac{1}{2}\left\{E\left[F^2(\rho)\right]-E\left[F^2(\rho)\cos 2\epsilon'\right]S_N(2\Delta')\right\}, \tag{A11}$$

$$\frac{1}{2N+1}\sum_{n=-N}^{N}\left\{E\left[F(\rho_n)\sin(\epsilon'_n+2\pi n\Delta')\right]\right\}^2$$
$$=\frac{1}{2N+1}\sum_{n=-N}^{N}E\left[F(\rho_n)\cos\epsilon'_n\right]^2\sin^2(2\pi n\Delta')$$
$$=\frac{1}{2}\left\{E\left[F(\rho)\cos\epsilon'\right]^2\left[1-S_N(2\Delta')\right]\right\}. \tag{A12}$$

Combining (A7) through (A12), we obtain

$$\operatorname{var}(\hat{\theta})\simeq\frac{\left\{E\left[F^2(\rho)\right]-\left(E\left[F(\rho)\cos\epsilon'\right]\right)^2\right\}\left[1-S_N(2\Delta')\right]+\left\{E\left[F^2(\rho)\right]-E\left[F^2(\rho)\cos 2\epsilon'\right]\right\}S_N(2\Delta')}{2m^2(2N+1)\left\{E\left[F(\rho)\cos\epsilon'\right]\right\}^2S_N^2(\Delta')}$$
$$\triangleq\frac{\Gamma(m,\Delta')}{(2N+1)\gamma}. \tag{A13}$$

Appendix B

Detailed Analysis of kth Power Nonlinearity (m even, k even, and $k\leqslant m-2$)

Let

$$x'_n+iy'_n=\rho^k e^{im(\theta+\epsilon)}$$

where $\rho e^{i\epsilon}=\sqrt{x_n^2+y_n^2}\,e^{i(\tan^{-1}(y_n/x_n)-\theta)}$ and $\zeta=\rho/\sigma$. (A14)

We have $p(\zeta,\epsilon)=\zeta e^{-(\zeta^2+\alpha^2)/2}e^{\zeta\alpha\cos\epsilon}$

$$E\left(\frac{\rho^{2k}}{\sigma^{2k}}\sin m\epsilon\right)=0 \tag{A15}$$

$$E\left(\frac{\rho^{2k}}{\sigma^{2k}}\sin^2 m\epsilon\right)=\frac{1}{2}E\left(\frac{\rho^{2k}}{\sigma^{2k}}\right)-\frac{1}{2}E\left(\frac{\rho^{2k}}{\sigma^{2k}}\right)\cos 2m\epsilon, \tag{A16}$$

where

$$E\left(\frac{\rho^{2k}}{\sigma^{2k}}\right)=E(\zeta^{2k})$$
$$=\int_0^\infty\zeta^{2k+1}\exp\frac{-(\zeta^2+\alpha^2)}{2}I_0(\alpha\zeta)\,d\zeta$$
$$=e^{-\gamma/2}\int_0^\infty\zeta^{2k+1}\exp\left(-\zeta^2/2\right)J_0(j\alpha\zeta)\,d\zeta,$$

where $\gamma=\alpha^2$.

Gradshteyn and Ryzhik [7, eq. (6.643.4)] yields

$$E(\zeta^{2k})=\frac{1}{2}k!\left(\frac{1}{2}\right)^{k-1}\sum_{m=0}^{k}\binom{k}{k-m}\frac{\left(\frac{\gamma}{2}\right)^m}{m!}$$
$$=2^k k!\sum_{m=0}^{k}\binom{k}{k-m}\frac{\left(\frac{\gamma}{2}\right)^m}{m!}$$
$$=\sum_{m=0}^{k}\binom{k}{k-m}^2(k-m)!\gamma^m 2^{k-m}.$$

Letting $n = k - m$ we obtain

$$E\left(\frac{\rho^{2k}}{\sigma^{2k}}\right) = \sum_{n=0}^{k}\binom{k}{n}^2 \gamma^{k-n} 2^n n! \tag{A17}$$

and

$$\begin{aligned} E&\left[\frac{\rho^{2k}}{\sigma^{2k}}\cos 2\epsilon'\right] \\ &= [\zeta^{2k}\cos 2\epsilon'] \\ &= \int_0^\infty \zeta^{2k+1}\exp\frac{-(\zeta^2+\alpha^2)}{2}\int_0^{2\pi}\cos 2m\epsilon e^{\zeta\alpha\cos\epsilon}\,d\epsilon\,d\zeta \\ &= e^{-\alpha^2/2}\int_0^\infty \zeta^{2k+1}e^{-\zeta^2/2}I_{2m}(\alpha\zeta)\,d\zeta \\ &= 2^k e^{-\gamma/2}\int_0^\infty x^k e^{-x} I_{2m}\left(\sqrt{2\gamma x}\right)dx \qquad \text{with } \gamma = \alpha^2. \end{aligned}$$

Gradshteyn and Ryzhik [7, eq. (6.643.2)] implies

$$E\left[\frac{\rho^{2k}}{\sigma^{2k}}\cos 2\epsilon'\right] = 2^k e^{-\gamma/2}\frac{\Gamma(k+m+1)}{\Gamma(2m+1)}\sqrt{\frac{2}{\gamma}} \cdot e^{\gamma/4}M_{-(k+1/2),m}\left(\frac{\gamma}{2}\right), \tag{A18}$$

where M is the Mathieu function. From Abramowitz and Stegun [8, eq. (13.1.32)] we can express this in terms of the confluent hypergeometric function

$$M_{-(k+1/2),m}\left(\frac{\gamma}{2}\right) = e^{-\gamma/4}\left(\frac{\gamma}{2}\right)^{1/2+m} M\left(m+k+1, 2m+1, \frac{\gamma}{2}\right). \tag{A19}$$

Therefore,

$$E\left(\frac{\rho^{2k}}{\sigma^{2k}}\cos 2\epsilon'\right) = 2^k e^{-\gamma/2}\left(\frac{\gamma}{2}\right)^m \frac{\Gamma(k+m+1)}{\Gamma(2m+1)} \cdot M\left(m+k+1, 2m+1, \frac{\gamma}{2}\right). \tag{A20}$$

Finally, from Abramowitz and Stegun, [8, eq. (13.5.1)],

$$\begin{aligned} &\frac{M\left(m+k+1, 2m+1, \frac{\gamma}{2}\right)}{\Gamma(2m+1)} \\ &= \frac{(-1)^{m+k+1}\left(\frac{2}{\gamma}\right)^{m+k+1}}{\Gamma(m-k)} \cdot \sum_{n=0}^{\infty}\frac{(m+k+1)_n(1+k-m)_n}{n!}\left(\frac{-2}{\gamma}\right)^n \\ &\quad + \frac{e^{\gamma/2}\left(\frac{2}{\gamma}\right)^{m-k}}{\Gamma(m+k+1)}\sum_{n=0}^{\infty}\frac{(m-k)_n(-(m+k))_n\left(\frac{2}{\gamma}\right)^n}{n!} \end{aligned} \tag{A21}$$

For m, k integers,

$$(m+k+1)_n = (m+k+1)(m+k+2)\cdots(m+k+n)$$

and

$$\begin{aligned} (1+k-m)_n &= (k-m+1)(k-m+2)\cdots(k-m+n) \\ &= (-1)^n(m-k-1)(m-k-2)\cdots(m-k-n), \end{aligned}$$

for $n \leqslant m-k-1$.

Therefore,

$$(m+k+1)_n(1+k-m)_n = (-1)^n\frac{(m+k+n)!}{(m+k)!}\frac{(m-k-1)!}{(m-k-n-1)!} \qquad (0 \leqslant n \leqslant m-k-1). \tag{A22}$$

Similarly,

$$(m-k)_n = (m-k)(m-k+1)\cdots(m-k+n-1), \qquad \text{for } k \leqslant m-1$$

and

$$\begin{aligned} (-(m+k))_n &= (-m-k)(-m-k+1)\cdots(-m-k+n-1) \\ &= (-1)^n(m+k)(m+k-1)\cdots(m+k+1-n), \end{aligned} \qquad \text{for } n \leqslant m+k.$$

Thus

$$(m-k)_n(-(m+k))_n = (-1)^n\frac{(m-k+n-1)!}{(m-k-1)!}\frac{(m+k)!}{(m+k-n)!} \qquad (0 \leqslant n \leqslant m+k, k \leqslant m-1), \tag{A23}$$

Therefore, using (A21), (A22), and (A23), we have

$$\begin{aligned} &\frac{M\left(m+k+1, 2m+1, \frac{\gamma}{2}\right)}{\Gamma(2m+1)} \\ &= (-1)^{m+k+1}\left(\frac{2}{\gamma}\right)^{m+k+1} \cdot \sum_{n=0}^{m-k-1}\frac{(m+k+n)!}{(m+k)!(m-k-n-1)!n!}\left(\frac{2}{\gamma}\right)^n \\ &\quad + e^{\gamma/2}\left(\frac{2}{\gamma}\right)^{m-k}\sum_{n=0}^{m+k}\frac{(m-k+n-1)!}{(m-k-1)!(m+k-n)!n!}\left(\frac{-2}{\gamma}\right)^n, \end{aligned} \tag{A24}$$

so that combining (A18) and (A24), we obtain

$$\begin{aligned} E&\left(\frac{\rho^{2k}}{\sigma^{2k}}\cos 2\epsilon'\right) \\ &= 2^k\left(\frac{\gamma}{2}\right)^k\sum_{n=0}^{m+k}\frac{(m+k)!(m-k+n-1)!}{(m+k-n)!(m-k-1)!n!}\left(\frac{-2}{\gamma}\right)^n \\ &\quad + (-1)^{m+k+1}2^k e^{-\gamma/2}\left(\frac{2}{\gamma}\right)^{k+1} \cdot \sum_{n=0}^{m-k-1}\frac{(m+k+n)!}{(m-k-n-1)!n!}\left(\frac{2}{\gamma}\right)^n \\ &= \gamma^k\sum_{n=0}^{m+k} n!\binom{m+k}{n}\binom{m-k+n-1}{n}\left(\frac{-2}{\gamma}\right)^n \\ &\quad + (-1)^{m+k+1}2^k e^{-\gamma/2}\left(\frac{2}{\gamma}\right)^{k+1} \cdot \sum_{n=0}^{m-k-1}\binom{m+k+n}{n}\frac{(m+k)!}{(m-k-n-1)!}\left(\frac{2}{\gamma}\right)^n. \end{aligned} \tag{A25}$$

We also need $E((\rho^k/\sigma^k)\cos\epsilon')$ for the expressions (5) and (8), but this satisfies the same equation as long as $m+k$ is even.

ACKNOWLEDGMENT

The authors express their appreciation for numerous constructive suggestions, which led to improvements on various phases of the manuscript, to Dr. Marvin Simon of JPL and to Professor George L. Turin of University of California, Berkeley. The junior author also gratefully acknowledges the role of the latter as her M.S. research advisor on the project which formed the nucleus of this work.

REFERENCES

[1] I. Gurantz, S. Blake, E. Hoversten, and J. Petranovich, "A high performance multiple data rate burst modem for satellite packet communication," EASCON Conference Record, Nov. 1981.
[2] C. Heegard, J. A. Heller, and A. J. Viterbi, "A microprocessor-based PSK modem for packet transmission over satellite channels," *IEEE Trans. Commun.*, vol. COM-26 no. 5 pp. 552–564, May, 1978.
[3] A. J. Viterbi, *Principles of Coherent Communication*. New York: McGraw-Hill, 1966.
[4] G. C. Clark, Jr., and J. B. Cain, *Error-Correction Coding for Digital Communication*. New York: Plenum Press, 1981.
[5] A. J. Viterbi and J. K. Omura, *Principle of Digital Communication and Coding*. New York: McGraw-Hill, 1979.
[6] J. J. Stiffler, *Theory of Synchronous Detection*. Englewood Cliffs, NJ: Prentice-Hall, 1971, p. 247.
[7] I. S. Gradshteyn and I. M. Ryzhik, *Table of Integrals, Series, and Products*. New York: Academic, 1965.
[8] M. Abramowitz and I. A. Stegun, Eds., *Handbook of Mathematical Functions*. Washington, DC: National Bureau of Standards, 1964.

On the Shape of a Set of Points in the Plane

HERBERT EDELSBRUNNER, DAVID G. KIRKPATRICK, AND RAIMUND SEIDEL

Abstract—**A generalization of the convex hull of a finite set of points in the plane is introduced and analyzed. This generalization leads to a family of straight-line graphs, "α-shapes," which seem to capture the intuitive notions of "fine shape" and "crude shape" of point sets. It is shown that α-shapes are subgraphs of the closest point or furthest point Delaunay triangulation. Relying on this result an optimal $O(n \log n)$ algorithm that constructs α-shapes is developed.**

I. INTRODUCTION

THE efficient construction of convex hulls for finite sets of points in the plane is one of the most exhaustively examined problems in the rather young field often referred to as "computational geometry." Part of the motivation is theoretical in nature. It seems to stem from the fact that the convex hull problem, like sorting, is easy to formulate and visualize. Furthermore, the convex hull problem, again like sorting, plays an important role as a component of a large number of more complex problems. Nevertheless, much of the work on convex hulls is motivated by direct applications in some of the more practical branches of computer science.

Manuscript received Sept. 9, 1981; revised June 1982. Preliminary results from this work were presented at the Conference on Graph Theory in Linz, June 1981. The work was supported by the National Sciences and Engineering Research Council of Canada, Grant A3583.

H. Edelsbrunner is with the Technical University of Graz, Institute fuer Informationsverarbeitung, Schiesstattgasse 4a, A-8010 Graz, Austria.

D. G. Kirkpatrick and R. Seidel are with the University of British Columbia, Department of Computer Science, 2075 Wesbrook Mall, Vancouver, BC, V6T 1W5 Canada.

Akl and Toussaint [1], for instance, discuss the relevance of the convex hull problem to pattern recognition. By identifying and ordering the extreme points of a point set, the convex hull serves to characterize, at least in a rough way, the "shape" of such a set. Jarvis [9] presents several algorithms based on the so-called nearest neighbor logic that compute what he calls the "shape" of a finite set of points. The "shape," in Jarvis' terminology, is a notion made concrete by the algorithms that he proposes for its construction. Besides this lack of any analytic definition, the inefficiency of Jarvis' algorithms to construct the "shape" is a striking drawback. More recently, Fairfield [6] introduced a notion of the shape of a finite point set based on the closest point Voronoi diagram of the set. He informally links his notion of shape with human perception but presents no concrete properties of his shapes, in particular, no algorithmic results. (See also Toussiant [20] for another definition of the shape of a set based on the Voronoi diagram.)

In this article, we introduce the notion of the "α-shape" of a finite set of points, for arbitrary real α. This notion is derived from a straightforward generalization of one common definition of the convex hull. Optimal algorithms for the construction of α-shapes and certain related structures are described. Consideration is given to the efficient construction of the α-shapes of a point set for several α's. The efficiency of our algorithms, in addition to other nice properties of α-shapes, leads us to believe that the family of

0018-9448/83/0700-0551$01.00 ©1983 IEEE